Interconversion of mechanical and dielectrical relaxation measurements for dicyclohexylmethyl-2-methyl succinate

R. Díaz-Calleja,* A. Garcia-Bernabé, and M. J. Sanchis
Departamento de Termodinámica Aplicada, Universidad Politécnica de Valencia, Valencia E-46071, Spain

L. F. del Castillo
Instituto de Investigaciones en Materiales, UNAM, Ap. Postal 70-360, Coyoacán, México DF, 04510, México
(Received 21 June 2005; published 18 November 2005)

A comparison between results of dielectrical relaxation and dynamic mechanical spectroscopies is carried out for the α-relaxation of the ester dicyclohexyl methyl-2-methyl succinate (DCMMS). The results for the dielectric permittivity and the shear modulus measurements are presented according to the empirical Havriliak-Negami (HN) equation. By using the time-temperature principle a master curve in each case was obtained for several temperatures. The comparative analysis presented here is based on the assumption of a relationship between rotational and shear viscosities. The former one is associated to the dielectrical relaxation, whereas the latter is associated to mechanical relaxation. Both viscosities are not necessarily equal in general, and we assume that the difference between them is an important factor to appropriately compare the dielectrical and mechanical results.

DOI: 10.1103/PhysRevE.72.051505 PACS number(s): 61.20.Lc, 77.22.Ch, 83.60.Fg

I. INTRODUCTION

The response function of dielectrical material to an oscillatory electric field is usually represented by the normalized dielectric permittivity

$$R^*(\omega) = \frac{\varepsilon^*(\omega) - \varepsilon_\infty}{\varepsilon_0 - \varepsilon_\infty} = \frac{1}{1 + i\omega\tau_D^*(\omega)}. \quad (1)$$

The quantities ε_0 and ε_∞ are the relaxed and unrelaxed dielectric constant, respectively. To obtain an expression for the complex relaxation time $\tau_D^*(\omega)$, DiMarzio and Bishop [1] (DB) proposed a prescription in which the Debye rotational frictional coefficient of a dipole particle is expressed in terms of the shear viscosity. This means that the relaxation of the electric polarization is governed by the same mechanism of the stress relaxation. In that sense, the Maxwell model for mechanical relaxation was used to represent the dielectric relaxation in terms of shear stress relaxation time, which is equal to the viscosity divided by the infinite frequency shear modulus (G_∞), namely $\tau_D \propto \tau_s = \eta_0 / G_\infty$. The second assumption of the DB model is to keep valid the proportionality between $\tau_D^*(\omega)$ and the shear viscosity $\eta_0^*(\omega)$ for all frequencies within the dielectrical relaxation domain. Therefore,

$$R^*(\omega) = \frac{1}{1 + i\omega A\, \eta_0^*(\omega)} \quad (2)$$

where A is the DB coefficient given by

$$A = \frac{4\pi r^3}{kT} \frac{\varepsilon_0 + 2}{\varepsilon_\infty + 2} \quad (3)$$

where r is the radius of the rotating dipole particles and k is the Boltzmann constant.

The DB equation is a generalization of the Debye theory [2]. The nonexponential decay of the dielectrical permittivity or the skewed arc of the Cole-Cole plot is provided by the frequency dependence on the dynamic viscosity. Considering a value of the radius of the rotating unit, this equation is not able to fit experimental data. However, it has been shown that the DB model qualitatively describes the physics underlying the interrelation between viscoelastic and dielectric relaxation data [3]. Along these lines contribution papers have considered the DB model in the same way as Eq. (2) [4–6].

Recently, dielectrical and mechanical moduli have been used in order to compare both type of measurements. Different definitions of the dielectrical modulus have been used. Christensen and Olsen have defined the electrical modulus in terms of the inverse of the complex dielectric susceptibility [7].

$$G_e^*(\omega) = \frac{1}{\varepsilon^*(\omega) - 1}. \quad (4)$$

Another definition of this modulus is given taking into account Ref. [8], namely

$$G_e^*(\omega) = \frac{1}{\varepsilon^*(\omega) - \varepsilon_\infty}. \quad (5)$$

The use of this equation leads to an inconsistency in the high frequency limit, since the real and imaginary parts of this electrical modulus diverge in this limit $\omega \to \infty$. The same is true for the shear compliance.

To avoid that problem, ε_∞ is replaced by ε_i. Here ε_i is equal to the squared refraction index. However, in the comparison of the predicted modulus with mechanical measurements, deviations are presented and further testing is necessary (see Ref. [8]).

To obtain a further insight along these lines, we abandon the purpose of making a comparison between shear moduli

*Electronic address: rdiazc@ter.upv.es

or taking the respective compliances as compare quantities. We propose to compare viscosities with different physical origin as are the shear and rotational ones. The aim of the present paper lies in the understanding of the molecular relaxation in a viscous and supercooled liquid. That is, separating the characteristics of the translational microscopic diffusion from the microscopic rotational diffusion. In fact, it has been assessed that the molecular rotation follows a different dynamic regime as the temperature is lowered toward the glass transition, in particular, when a crossover dynamic of fragile glass formers [9] is reached above the glass transition temperature around $T_C=1.2T_g$. Several models and the experimental results suggest that the decoupling between rotational diffusion and viscosity is present together the heterogeneity dynamics [10]. This effect was related to the breakdown of the Debye-Stokes-Einstein (DSE) relation for the translational diffusion coefficient [11,12]. The characterization of this relation implies the diffusion coefficient scales shear viscosity as a power law, with an exponent in the range between zero and one, depending on the material [13,14].

Following these findings, we propose to introduce a scaling relationship between real and imaginary parts of the shear and rotational viscosities. In this paper, we will try to show that in making this assumption it is possible to find a way to compare mechanical and dielectrical measuring.

II. THE HAVRILIAK-NEGAMI REPRESENTATION FOR EXPERIMENTAL MECHANICAL AND DIELECTRICAL DATA

The dielectrical and mechanical measurements were done at the laboratory of N. B. Olsen in IMFUFA, Roskilde University Center, Denmark. The mechanical measurement were carried out at different temperatures using a piezoelectric transducer cell, enabling one to measure the complex shear modulus in the frequency interval from 10^{-2} Hz to 10^{2} kHz. For the dielectrical measurement, a HP4192A impedance analyzer was used in the same frequency interval. The experimental cell, temperature controller, and procedure to collect data were described previously [15]. The glass transition temperature T_g of this glass forming liquid is 220 K as previously reported [16].

The complex dielectrical permittivity and mechanical modulus were characterized employing the empirical Havriliak-Negami (HN) equation [17].

Thus, for dielectrical relaxation this model is given by

$$\frac{\varepsilon^{*}-\varepsilon_{\infty}}{\varepsilon_0-\varepsilon_{\infty}}=\frac{1}{[1+(i\omega\tau_D)^{\alpha}]^{\beta}} \tag{6}$$

where α and β are the former parameters and τ_D represents the relaxation time.

For the complex shear modulus the HN representation is given by

$$\frac{G_s^{*}-G_s(\infty)}{G_0-G_s(\infty)}=\frac{1}{[1+(i\omega\tau_s)^{\gamma}]^{\delta}} \tag{7}$$

where $G_s(\infty)$ is the unrelaxed shear modulus, G_0 is the relaxed shear modulus, γ and δ are the former parameters, and τ_s represents the relaxation time.

TABLE I. Parameters of Havriliak-Negami equation for dielectrical measurements.

T (K)	ε_{∞}	$\varepsilon_0-\varepsilon_{\infty}$	α	β	τ_D (s)
218	2.110	4.780	0.82	0.50	3.9
220	2.140	4.650	0.85	0.48	1.0
222	2.160	4.520	0.84	0.48	2.3×10^{-1}
224	2.200	4.530	0.85	0.48	1.0×10^{-1}
226	2.210	4.520	0.84	0.48	3.2×10^{-2}
228	2.179	4.456	0.90	0.41	8.0×10^{-3}
230	2.162	4.441	0.92	0.40	2.8×10^{-3}
232	2.168	4.410	0.91	0.39	1.1×10^{-3}
234	2.147	4.403	0.92	0.38	4.5×10^{-4}
238	2.114	4.380	0.91	0.38	1.1×10^{-4}
242	1.942	4.496	0.93	0.34	2.8×10^{-5}
246	1.485	4.895	0.94	0.29	8.0×10^{-6}

The HN parameters at different temperatures for dielectrical and mechanical measurements are given in Tables I and II, respectively.

The values of $\log_{10}(\tau_D)$ and $\log_{10}(\tau_s)$ versus inverse of temperature are represented in Fig. 1. We observe that, independently of temperature, the average shift between two curves is about 0.6. This constant shift is associated to the time delay between the mechanical and dielectric responses.

The time-temperature superposition principle can be applied to mechanical and dielectric results. Considering a special frequency domain to avoid deviations of the data at high frequencies, a master curve is obtained. Thus, in Figs. 2 and 3 we have represented ε', ε'', G' and G'' versus $(a_T f)$, where a_T represents the temperature-dependent scaling factor for the frequencies.

The dependence of a_T with the temperature was analyzed using the Williams, Landel, and Ferry (WLF) equation,

$$\log(a_T)=\frac{-C_1(T-T_0)}{C_2+(T-T_0)}. \tag{8}$$

TABLE II. Parameters of Havriliak-Negami equation for mechanical measurements.

T (K)	$10^{-8}G_s(\infty)$ (Pa)	$10^{-8}(G_s(\infty)-G_0)$ (Pa)	γ	δ	τ_s (s)
208	8.88	8.88	0.92	0.29	7.9×10^{-1}
220	8.71	8.70	0.96	0.26	2.3×10^{-1}
222	8.39	8.41	0.91	0.28	5.7×10^{-2}
224	8.27	8.29	0.90	0.27	1.7×10^{-2}
226	8.15	8.17	0.91	0.26	5.9×10^{-3}
228	8.47	8.48	0.92	0.23	2.3×10^{-3}
230	8.38	8.38	0.93	0.22	9.2×10^{-4}
232	8.50	8.50	0.92	0.21	3.7×10^{-4}
234	8.87	8.87	0.93	0.19	1.7×10^{-4}
238	8.89	8.91	0.89	0.19	3.6×10^{-5}

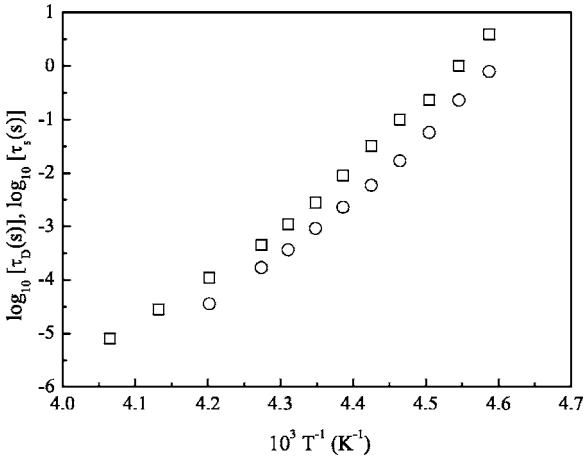

FIG. 1. Temperature dependence of dielectrical (□) and mechanical (○) relaxation time.

The fitting parameters C_1 and C_2 are 11.5 and 54.3 for dielectrical spectroscopy and 11.8 and 54.9 for mechanical spectroscopy, at reference temperature (T_0) of 228 K.

III. THE RELATIONSHIP BETWEEN ROTATIONAL AND SHEAR VISCOSITIES

A. Rotational viscosity

Dynamic dielectrical permittivity of a condensed system of molecules with permanent electric dipole moment can be represented by the following equation [18]

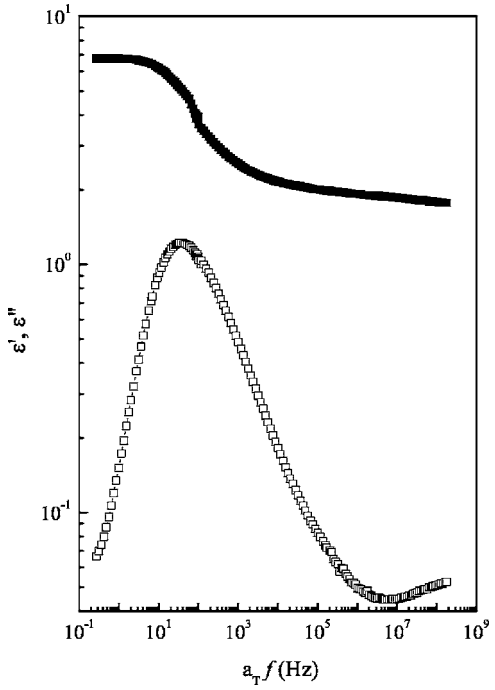

FIG. 2. Master-type plot of the dielectrical measurement at 228 K, real part (■) and imaginary part (□).

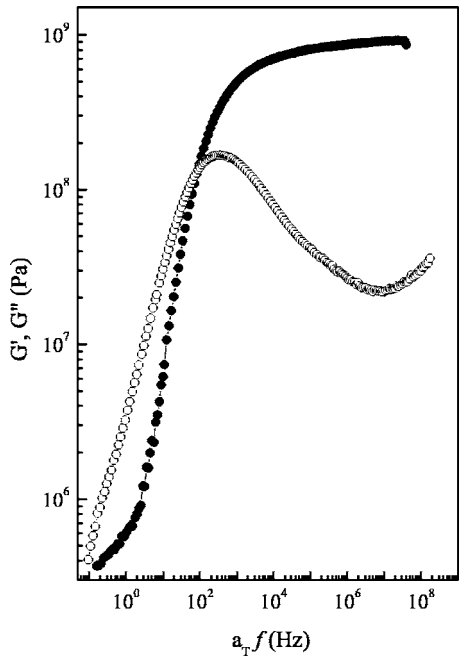

FIG. 3. Master-type plot of the mechanicalal measurement at 228 K, real part (●) and imaginary part (○).

$$R^*(\omega) = \frac{1}{1 - \frac{\omega^2}{\omega_T^2} + i\omega\left[\frac{\varepsilon_0 + 2}{\varepsilon_\infty + 2}\right]\tau_R^*(\omega)} \tag{9}$$

where τ_R^* is the rotational relaxation time, $[(\varepsilon_0+2)/(\varepsilon_\infty+2)]$ is the field factor correction and ω_T is the resonance frequency.

Now the inertial effects are neglected. This is due to the fact that the dielectrical relaxation under study lies far from resonance frequency, that is $\omega_T^2 \gg \omega^2$. Then Eq. (9) is reduced to [19]

$$R^*(\omega) = \frac{1}{1 + i\omega\left[\frac{\varepsilon_0 + 2}{\varepsilon_\infty + 2}\right]\tau_R^*(\omega)}. \tag{10}$$

The rotational relaxation time can be done in terms of the complex rotational diffusion coefficient, defined via the torques acting on a rotating sphere [20]. According to the fluctuation-dissipation theorem it can be expressed as

$$\tau_R^*(\omega) = \frac{1}{2D^*(\omega)} = \frac{\xi^*(\omega)}{2kT}. \tag{11}$$

Taking into account the situation of a large sphere within a fluid and by using the continuum approach, the frictional coefficient can be given by

$$\xi = 8\pi r^3 \eta_0. \tag{12}$$

It should be noted that Eq. (12) has been derived at a macroscopic level. This means that this equation cannot be necessarily applied on the length scale of molecular dimensions, in which the rotational nature prevails. That is, the frictional coefficient expresses the opposition of the sur-

rounding fluid to the rotational motion of the dipole particle. This is produced by the torque induced by the interaction dipole-electric field. The important point is that this shear viscosity is not necessarily equal to the rotational one. In particular, the frictional coefficient could depend on the boundary conditions of the surrounding fluid [21,22]. This should be the case of supercooled fluids near the glass transition temperature by considering that any dipole is inserted in a cooperatively rearranging region. Therefore, Eq. (12) should be modified to consider the rotational viscosity instead of the shear viscosity [23] to give

$$\xi^* = 8\pi r^3 \eta_0^*. \tag{13}$$

Substitution of Eqs. (13), (11), and (10) into Eq. (9) leads to

$$R^*(\omega) = \frac{1}{1 + i\omega A\, \eta_{\mathrm{rot}}^*(\omega)} \tag{14}$$

Here A is the same quantity as given in Eq. (2). Equation (14) is the modified DB equation, and therefore, the actual viscosity related to the electric susceptibility might correspond to the rotational one. The corresponding evaluation from dielectrical measurements can be done by using the next algorithm obtained from Eqs. (10) and (11).

$$\eta_{\mathrm{rot}}^*(\omega) = \frac{1}{i\omega A}\left[\frac{1}{R^*(\omega)} - 1\right]. \tag{15}$$

At this point, it should be mentioned that the product $A\,\eta_{\mathrm{rot}}^*(\omega)$ corresponds to the second-order memory function, whose properties are described elsewhere [16,24].

B. The shear viscosity

The dynamic shear viscosity or the translational one is obtained from the dynamic shear modulus by

$$\eta_{\mathrm{trans}}^*(\omega) = \frac{G_s^*(\omega)}{i\omega}. \tag{16}$$

The real and imaginary parts of the dynamic shear viscosity are given in terms of the frequency according to the following definition:

$$\eta_{\mathrm{trans}}^*(\omega) = \eta'_{\mathrm{trans}}(\omega) - i\,\eta''_{\mathrm{trans}}(\omega). \tag{17}$$

Preliminary calculation of the radius in Eq. (3) (unpublished results) gives $R = 8$ Å. From this value the parameter A can be estimated given nearly $4.3 \cdot 10^{-6} (m^3/\mathrm{K}\cdot\mathrm{mol})$.

Similarly, for the dynamic rotational viscosity one has

$$\eta_{\mathrm{rot}}^*(\omega) = \eta'_{\mathrm{rot}}(\omega) - i\,\eta''_{\mathrm{rot}}(\omega). \tag{18}$$

The evaluation of these functions is made by using experimental data in Eqs. (15) and (16), and the results are shown in Figs. 4 and 5. Real parts of dynamic viscosities tend to be nearly constant at low frequency. These limiting values are the zero-rotational rate $\eta_{\mathrm{rot}}(0)$ and the zero-shear rate $\eta_{\mathrm{trans}}(0)$ viscosities. These values are reported as a function of the temperature in Table III. In the same way as in the dielectric and mechanical results, the time-temperature superposition principle is applied for zero-rotational rate and

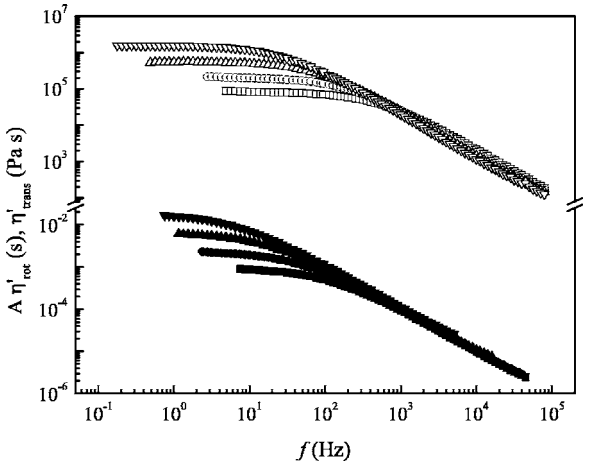

FIG. 4. Variation of real part of dynamic shear (open) and rotational (solid) viscosity, (□) 226, (○) 228, (△) 230, and (▽) 232 K.

zero-shear rate viscosities. The WLF equation for this case is as follows

$$\log_{10}(a'_T) = \frac{\eta_T(0)}{\eta_{T_0}(0)} = \frac{-D_1(T - T_0)}{D_2 + (T - T_0)}. \tag{19}$$

The values of constants D_1 and D_2 are 11.9 and 54.2, respectively, for zero-rotational rate viscosity and 11.5 and 53.4 for zero-shear rate viscosity at 228 K as reference temperature. The values of $\log_{10}[a'_T(\mathrm{rot})]$ and $\log_{10}[a'_T(\mathrm{trans})]$ versus inverse of temperature are presented in Fig. 6.

Imaginary parts of dynamic viscosities are characterized by the presence of maxima, which coincides with the end of a relative plateau in the real part. The temperature dependence of the shift of these curves can also be studied by time-temperature superposition principle, Eq. (19). The values of new constants D_1 and D_2 are, respectively, 12.6 and 56.7 for maximum rotational viscosity and 12.0 and 54.0 for maximum shear viscosity at 228 K as reference temperature. As we can see, the values of the constants D_1 and D_2 are

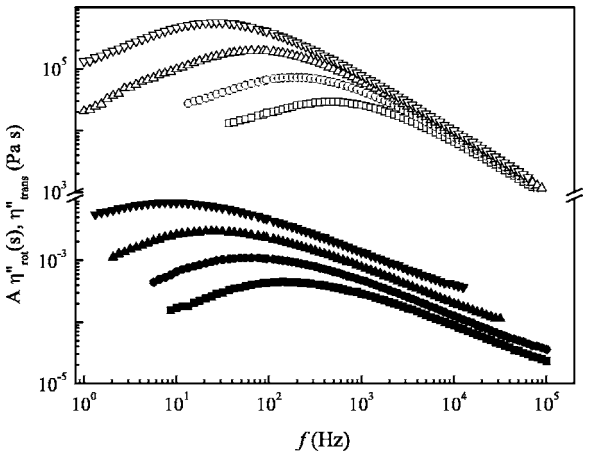

FIG. 5. Variation of imaginary part of dynamic shear (open) and rotational (solid) viscosity, (□) 226, (○) 228, (△) 230, and (▽) 232 K.

TABLE III. Zero-rotational rate and zero-shear rate viscosities.

T (K)	$A\,\eta'_{\mathrm{rot}}(0)$ (s)	$\eta'_{\mathrm{trans}}(0)$ (Pa s)
218		2.42×10^{8}
220		5.71×10^{7}
222		1.63×10^{7}
224	5.05×10^{-2}	4.93×10^{6}
226	1.74×10^{-2}	1.54×10^{6}
228	5.99×10^{-3}	5.52×10^{5}
230	2.28×10^{-3}	2.16×10^{5}
232	8.88×10^{-4}	8.30×10^{4}
234	3.87×10^{-4}	3.62×10^{4}
238	8.08×10^{-5}	7.88×10^{3}
242	2.17×10^{-5}	2.09×10^{3}
246	6.27×10^{-6}	6.55×10^{2}

very close for all the cases, and the same is true for dielectrical and mechanical master curves (see above).

In the next section we compare the real and imaginary parts of these viscosities.

C. Scaling relation between the rotational and shear viscosities

In order to introduce a scale relationship, we will consider that the rotational diffusion is related to the shear viscosity according to the DSE relation, namely

$$D_{\mathrm{rot}} = \frac{kT}{6\pi d^3}\frac{1}{\eta_{\mathrm{rot}}} \tag{20}$$

and

$$\eta_{\mathrm{rot}} = \eta_0. \tag{21}$$

These equalities are adequate for spherical particles of any radius rotating in a Newtonian fluid, as it is the prescription of the DSE relationship. However, for dipoles of the same size of the molecular fluid or dipoles in a viscoelastic fluid, as it is in the case of a supercooled liquid under nonergodic conditions, these results for the DSE relation break down. In this case, the relation between the rotational diffusion and the shear viscosity can be formulated in terms of a power law with a fractional exponent. A possible physical picture is that the shear motion facilitates molecular jumps-rotations over energy barriers according to the theory of rate processes of Eyring [25]. Furthermore this effect has been recognized as the decoupling of translational diffusion and the relaxation, as a consequence of the dynamic heterogeneity [10,26]. Therefore, this decoupling modifies the DSE relationship, and a fractional diffusion coefficient [27,28] was suggested as valid in the temperature interval $T_g < T < 1.2T_g$ [29]

$$D_{\mathrm{rot}} = \frac{kT}{6\pi d^3}\left(\frac{1}{\eta_0}\right)^{\zeta}. \tag{22}$$

The exponent in Eq. (22) depends on both the diffusing particle and the fluid, with values in the range of $0<\zeta\leqslant 1$. This result suggests proposing a relationship between viscosities in the following way:

$$\eta_{\mathrm{rot}} = B(\eta_0)^{\zeta}. \tag{23}$$

The generalization of this relationship for frequency-dependent viscosities gives after splitting the real and imaginary parts

$$\eta'_{\mathrm{rot}}(\omega) = B'(\eta'_{\mathrm{trans}})^{\zeta_1}, \tag{24}$$

$$\eta''_{\mathrm{rot}}(\omega) = B''(\eta''_{\mathrm{trans}})^{\zeta_2}. \tag{25}$$

These relationships can be verified using experimental data considering the prescriptions of Eqs. (15) and (16). $\mathrm{Log}_{10}-\log_{10}$ plots for the real and imaginary parts of the rotational viscosity versus the real and imaginary parts of the translational viscosity are shown in Figs. 7 and 8. In these figures we can observe a linear part at high frequencies and a non-

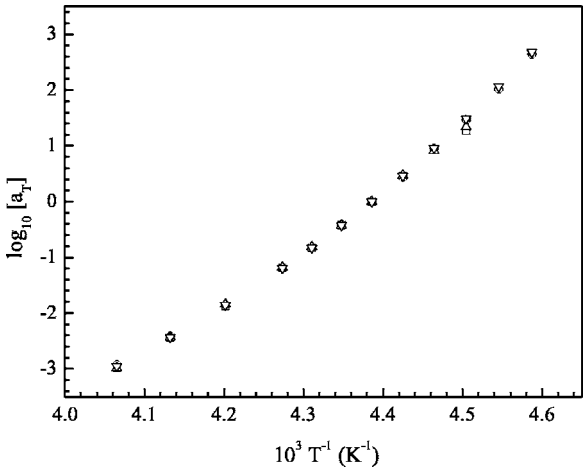

FIG. 6. Temperature dependence of the shift (a_T) for (□) zero-rotational rate viscosity, (○) zero-shear rate viscosity, (△) maximum of imaginary part of rotational viscosity, and (▽) maximum of imaginary part of shear viscosity.

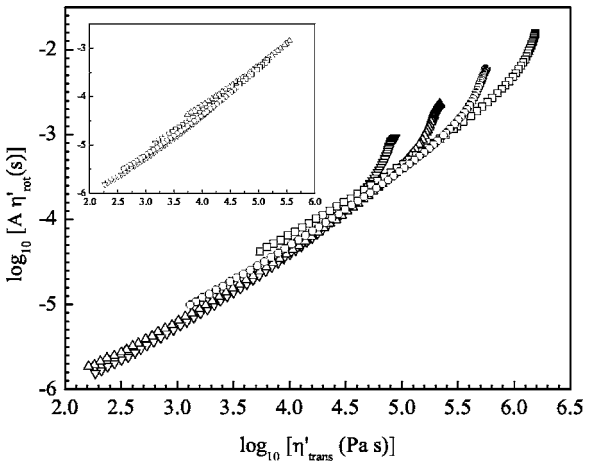

FIG. 7. $\log_{10}$ real part of dynamic shear vs $\log_{10}$ real part dynamic rotational viscosity [(□) 226, (○) 228, (△) 230, and (▽) 232 K]. Inset: linear behavior of relation between both viscosities.

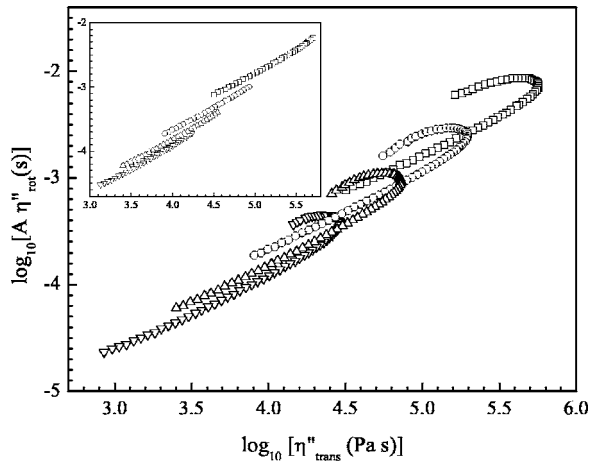

FIG. 8. $\log_{10}$ imaginary part of dynamic shear vs $\log_{10}$ imaginary part dynamic rotational viscosity [(□) 226, (○) 228, (△) 230, and (▽) 232 K]. Inset: Linear behavior of relation between both viscosities.

linear part at low frequencies. The slopes of the real and imaginary parts of the viscosities give the fractional exponents in a linear part of $\zeta_1=0.84\pm0.01$ and $\zeta_2=0.72\pm0.01$. The fractional exponents and pre-exponential factors as a temperature function are summarized in Table IV.

On the other hand, an alternative scaling relationship between the diffusion coefficient and the viscosity has been proposed in [30]

$$D_{\mathrm{rot}} \propto \left(\frac{T}{\eta_0}\right)^{\zeta}. \tag{26}$$

It leads to a scaling relationship between viscosities of the form

$$\eta^0_{\mathrm{rot}} = B'''\left(\frac{\eta_0}{T}\right)^{\zeta}. \tag{27}$$

However, this temperature contribution does not affect the scaling-power parameter, but modifies the temperature dependence of the B''' coefficient. However, the analysis goes on following the same form as we did above.

IV. DISCUSSION

We explore the possibility to convert electrical data obtained in the dielectrical spectroscopy into mechanical spectroscopy data.

TABLE IV. Exponent and pre-exponent factors of generalized DSE relations [Eqs. (24) and (25)].

T (K)	ζ_1	$10^8 B'$	ζ_2	$10^7 B''$
226	0.84	2.80	0.72	4.07
228	0.85	2.04	0.71	2.97
230	0.84	1.94	0.72	2.03
232	0.83	1.83	0.73	1.52

The procedure that we proposed is to look for a transformation between the dielectrical complex relaxation time $\tau^*_D(\omega)$ and the corresponding shear relaxation time $\tau^*_s(\omega)$. We have shown that this transformation can be established by considering a scaling relationship between the real and imaginary parts of the rotational and shear viscosity. According to the analysis presented here, at least one new scaling parameter is necessary in the formulation to get a quantitative prediction starting with mechanical or dielectrical measurements. We assume an interpretation of this scaling parameter related to the crossover dynamic regime in supercooled liquids around the glass transition. The result can be expressed in the form of the complex relaxation time

$$\tau^*_D(\omega) = B'(\eta'_{\mathrm{trans}}(\omega))^{\zeta_1} - iB''(\eta''_{\mathrm{trans}}(\omega))^{\zeta_2}. \tag{28}$$

Here, the complex relaxation time is given in terms of the real and imaginary parts of the complex shear viscosity, which can be obtained from the complex shear modulus using Eq. (16).

The relaxation time in Eq. (28) reduces to the DB form if $\zeta_1=\zeta_2=1$, which is the case when the Debye relaxation time is equal to the shear relaxation. Then according to Eq. (2) the coefficients $B'=B''$ and equal to A.

Apparently, from the results presented here, it seems that the values of the scaling parameters ζ_1 and ζ_2 do not equal each other, and their difference should be temperature dependent without a violation of the causality principle in the Kramers-Kronig formulation (see Appendix A). However, to establish this difference from experimental results is a matter of future investigation and the conclusions presented here need to be contrasted with data from a different glass forming system.

Finally, theoretical models are lacking to evaluate the scaling parameters. Similarly, it remains a physical explanation of Eq. (28).

ACKNOWLEDGMENTS

This work was supported by the CICYT through Grant No. MAT2002-04042-C02-01. One of the authors (L.F. del Castillo) wishes to acknowledge financial support from SEP-CONACYT grant 2004–C01–47070 and DGAPA-UNAM, Project IN-107502. A. G.-B. wants to thank the Spanish Ministry of Education and Science for research contract (Programa Ramón y Cajal). The authors especially thank Professor Niels Boye Olsen from Roskilde Universitetcenter (Denmark) for dielectrical and mechanical measurements.

APPENDIX A: THE KRAMERS-KRONING RELATIONS FOR DYNAMIC VISCOSITIES

The real and imaginary parts of the shear viscosity are given by

$$\eta'_{\mathrm{trans}}(\omega) = \frac{G''_s(\omega)}{\omega}, \tag{A1}$$

$$\eta''_{\mathrm{trans}}(\omega) = \frac{G'_s(\omega)}{\omega}. \tag{A2}$$

On the other hand, the real and imaginary parts of the rotational viscosity are expressed by

$$\eta'_{\mathrm{rot}}(\omega) = B'(\eta'_{\mathrm{trans}})^{\zeta_1}, \tag{A3}$$

$$\eta''_{\mathrm{rot}}(\omega) = B''(\eta''_{\mathrm{trans}})^{\zeta_2}. \tag{A4}$$

Particularly, by using the Kramers-Kronig relations for the next complex quantities $\eta^*_{\mathrm{rot}}(\omega)$, $\eta^*_{\mathrm{trans}}(\omega)$, and $G^*_s(\omega)$ the following expressions are obtained:

$$G''_s(\omega) = -\frac{\pi}{2}\frac{dG'_s}{d\ln\omega}, \tag{A5}$$

$$\eta''_{\mathrm{rot}}(\omega) = -\frac{\pi}{2}\frac{d\eta'_{\mathrm{rot}}}{d\ln\omega}, \tag{A6}$$

$$\eta''_{\mathrm{trans}}(\omega) = -\frac{\pi}{2}\frac{d\eta'_{\mathrm{trans}}}{d\ln\omega}. \tag{A7}$$

We propose to take Eq. (A3) as the starting point and we obtain Eq. (A4).

We assume that the real and imaginary parts of the shear modulus in the high frequency wing are given by power functions

$$G'_s = M_1\omega^m, \tag{A8}$$

$$G''_s = M_2\omega^n. \tag{A9}$$

Applying the operator

$$-\frac{\pi}{2}\frac{d}{d\ln\omega} \tag{A10}$$

of both sides of Eq. (A3), results

$$\eta''_{\mathrm{rot}}(\omega) = -\frac{\pi}{2}\frac{d\eta'_{\mathrm{rot}}(\omega)}{d\ln\omega} = -\frac{\pi}{2}\frac{d}{d\ln\omega}B'(\eta'_{\mathrm{trans}})^{\zeta_1}, \tag{A11}$$

$$\eta''_{\mathrm{rot}}(\omega) = -B'\zeta_1(\eta'_{\mathrm{trans}})^{\zeta_1-1}\frac{\pi}{2}\frac{d\eta'_{\mathrm{trans}}}{d\ln\omega} = B'\zeta_1(\eta'_{\mathrm{trans}})^{\zeta_1-1}\eta''_{\mathrm{trans}}. \tag{A12}$$

Now, using the Eqs. (A8) and (A9) as well as Eq. (16) the following relations are obtained:

$$\eta'_{\mathrm{trans}}(\omega) = \left(\frac{M_2}{M_1^{\Delta}}\right)(\eta''_{\mathrm{trans}})^{\Delta}, \tag{A13}$$

$$\Delta = \frac{n-1}{m-1}. \tag{A14}$$

Replacing the above result into Eq. (A12) and comparing with the last result with Eq. (A4), the parameters ζ_2 and B'' can be identified as

$$\zeta_2 = 1 - \Delta(1-\zeta_1) \tag{A15}$$

and

TABLE V. Exponent and pre-exponent factors for real parts of dynamic viscosities.

T (K)	226	228	230	232
m_r	−0.990	−0.990	−0.978	−0.965
m_t	−1.164	−1.162	−1.168	−1.553
$10^1 B'_r$	6.54	5.95	5.01	3.91
$10^8 B'_t$	5.19	5.82	7.18	7.07
ζ_1 (calc)	0.85	0.85	0.84	0.83
$10^8 B'$ (calc)	3.04	2.07	1.96	1.84

$$B'' = B'\zeta_1\left(\frac{M_2}{M_1^{\Delta}}\right)^{\zeta_1-1}. \tag{A16}$$

As we can see, $\zeta_2=\zeta_1$, only of $m=n$ but this is not, in general, the case. It is noticed that it is not possible to obtain Eq. (A3) from Eq. (A4) following a procedure analogous to the former due to the fact that an equation does not exist which is similar to Eq. (A11) for the real part of the rotational viscosity.

APPENDIX B: EXPONENT AND PRE-EXPONENT FACTORS FOR REAL AND IMAGINARY PARTS OF DYNAMIC VISCOSITIES

The interconversion between the dynamic translational viscosity and dynamic rotational viscosity was realized at a high frequency, where the viscosities are decreased (Figs. 4 and 5). In this range, we can assume that whereas real parts of viscosities are given by power functions

$$\eta'_{\mathrm{rot}} = B'_r\omega^{m_r}, \tag{B1}$$

$$\eta'_{\mathrm{trans}} = B'_t\omega^{m_t}. \tag{B2}$$

From both equations, the following relation is obtained:

$$\eta'_{\mathrm{rot}} = \frac{B'_r}{[B'_t]^{(m_r/m_t)}}[\eta'_{\mathrm{trans}}]^{(m_r/m_t)} \tag{B3}$$

by comparison with Eq. (22), we determine the interconversion parameters from power functions parameters for dynamic viscosity.

TABLE VI. Exponent and pre-exponent factors for imaginary parts of dynamic viscosities.

T (K)	226	228	230	232
n_r	−0.533	−0.562	−0.582	−0.575
n_t	−0.736	−0.750	−0.780	−0.781
$10^0 B''_r$	1.46	1.03	0.78	0.49
$10^7 B''_t$	4.88	3.96	4.17	3.38
ζ_2 (calc)	0.72	0.75	0.75	0.74
$10^7 B''$ (calc)	3.97	2.09	1.62	1.42

$$B' = \frac{B'_r}{[B'_t]^{(m_r/m_t)}} \tag{B4}$$

and

$$\zeta_1 = \frac{m_r}{m_t}. \tag{B5}$$

By the same way in imaginary parts and assuming that the imaginary parts of dynamic viscosities are given by similar power functions

$$\eta''_{\text{rot}} = B''_r \omega^{n_r}, \tag{B6}$$

$$\eta''_{\text{trans}} = B''_t \omega^{n_t}. \tag{B7}$$

obtaining:

$$B'' = \frac{B''_r}{[B''_t]^{(n_r/n_t)}} \tag{B8}$$

and

$$\zeta_2 = \frac{n_r}{n_t}. \tag{B9}$$

We can observe that the values obtained by these two methods (see Tables IV–VI) are very close.

[1] E. A. Dimarzio and M. Bishop, J. Chem. Phys. **60**, 3802 (1974).
[2] R. Díaz-Calleja, E. Riande, and J. SanRoman, J. Polym. Sci., Part B: Polym. Phys. **31**, 711 (1993).
[3] R. Zorn, F. I. Mopsik, G. B. McKenna, L. Willner, and D. Richter, J. Chem. Phys. **107**, 3645 (1997).
[4] R. Díaz-Calleja, Polymer **19**, 235 (1978).
[5] D. Ferri and L. Castellani, Macromolecules **34**, 3973 (2001).
[6] J. Mijovic, Y. F. Han, M. Y. Sun, and S. Pejanovic, Macromolecules **36**, 4589 (2003).
[7] T. Christensen and N. B. Olsen, J. Non-Cryst. Solids **172**, 357 (1994).
[8] K. Niss and B. Jokobsen, Thesis/dissertation, Roskilde University (2003).
[9] H. Sillescu, J. Non-Cryst. Solids **243**, 81 (1999).
[10] S. C. Glotzer, V. N. Novikov, and T. B. Schroder, J. Chem. Phys. **112**, 509 (2000).
[11] C. DeMichele and D. Leporini, Phys. Rev. E **63**, 036702 (2001).
[12] M. T. Cicerone and M. D. Ediger, J. Chem. Phys. **104**, 7210 (1996).
[13] J. F. Douglas and D. Leporini, J. Non-Cryst. Solids **235**, 137 (1998).
[14] L. Andreozzi, M. Faetti, M. Giordano, and D. Leporini, J. Phys.: Condens. Matter **11**, A131 (1999).
[15] T. Christensen and N. B. Olsen, Rev. Sci. Instrum. **66**, 5019 (1995).
[16] R. Díaz-Calleja, A. García-Bernabé, M. J. Sanchis, and L. F. del Castillo, J. Chem. Phys. **113**, 11258 (2000).
[17] S. Havriliak and S. Negami, Polymer **8**, 161 (1967).
[18] R. Lobo, J. E. Robinson, and S. Rodriguez, J. Chem. Phys. **59**, 5992 (1973).
[19] L. F. del Castillo, R. Díaz-Calleja, A. Garcia-Bernabé, and M. J. Sanchis, J. Non-Cryst. Solids **307**, 288 (2002).
[20] T. W. Nee and R. Zwanzig, J. Chem. Phys. **52**, 6353 (1970).
[21] R. E. Rosenweig, *Ferrohydrodynamics* (Cambridge University Press, Cambridge, 1985).
[22] B. U. Felderhof, Physica A **84**, 569 (1976).
[23] B. Cichocki and B. U. Felderhof, Physica A **297**, 115 (2001).
[24] R. Díaz-Calleja, M. J. Sanchis, and L. F. del Castillo, J. Chem. Phys. **109**, 9057 (1998).
[25] C. DeMichele and D. Leporini, Phys. Rev. E **63**, 036701 (2001).
[26] S. C. Glotzer, J. Non-Cryst. Solids **274**, 342 (2000).
[27] F. Fujara, B. Geil, H. Sillescu, and G. Fleischer, Z. Phys. B: Condens. Matter **88**, 195 (1992).
[28] I. Chang, F. Fujara, B. Geil, G. Heuberger, T. Mangel, and H. Sillescu, J. Non-Cryst. Solids **172**, 248 (1994).
[29] E. Rossler, Phys. Rev. Lett. **65**, 1595 (1990).
[30] L. Andreozzi, M. Bagnoli, M. Faetti, and M. Giordano, J. Non-Cryst. Solids **303**, 262 (2002).